The effect of initial fuel temperature on vaporization in aero engine combustors with prevaporization

C. Hassa*, P.F. Wiesmath
Institute of Propulsion Technology, German Aerospace Center,
Linder Hoehe, 51147 Cologne, Germany

Abstract

In gas turbines, the temperature of liquid fuels influences atomization and evaporation and thus the position of the flame front which in turn influences almost every aspect of the combustion. Nevertheless little is known about the actual fuel temperature at the place of initial contact with the air. The paper describes an experimental investigation of atomization and evaporation of Kerosene sprays emitted from a jet in cross flow at operating conditions similar to an aero engine cruise and a variation of Kerosene temperature between 40 and 150°C. Phase Doppler Anemometry was used to measure drop size and velocity and to infer vaporization rates of the spray. A noticeable influence of the Kerosene temperature was measured. For the isothermal atomization with identical air and liquid temperatures and a variation between 40 and 150 °C, the Sauter diameter drops from 20 to 16 µm. For a residence time of 0.5 ms at 750 K air temperature, 9 bar air pressure and 120 m/s air velocity, the fuel temperature difference of 110 °C is responsible for 26 % higher vaporization. Hence the initial fuel temperature can affect combustion stability and efficiency at critical conditions, which makes it attractive to investigate the effect in realistic premixing combustors.

Introduction

Liquid fuels must be vaporized before combustion. Prior to vaporization the fuel must be heated up to a temperature near to the boiling temperature to achieve considerable vaporization rates. For partially premixed and prevaporized combustion of Kerosene in aeroengines, the compressor outlet temperature and the boiling temperature of the fuel constitute the driving temperature difference for the vaporization. Both rise with the pressure ratio of the engine cycle. With higher boiling temperatures, heating of the fuel requires a higher part of the overall energy needed for vaporization. Hence the fuel temperature at the injection point cannot be neglected. A higher fuel temperature also decreases surface tension, which upon atomization leads to smaller droplets further enhancing the vaporization rate. Since the vaporization time in the combustor is connected with a convection of the fuel, it influences the position of the flame, one of the most important overall features of the combustor impacting among others combustion stability, efficiency, soot formation and combustor thermo acoustics. Although these factors are known, the fuel temperature at the injection point usually is not and systematic information of its influence in practical combustors does not exist. This contribution therefore aims to provide information on the magnitude of this influence for combustors with prevaporization at realistic conditions.

In the airplane, the fuel is heated up on its way from the tank to the injector tip, often also in heat exchangers for oil cooling, and care must be taken not to overheat the fuel [1]. Aviation fuel consists of a wide band of molecules which may crack and, under the influence of the dissolved air, may build up coke in the fuel lines leading to uneven fuel distribution or full blockage of the fuel lines. There are no published values of industrial design limits; however experience at General Electric Aero Engines showed that coking can become a significant problem with wetted wall temperatures approaching 200 °C [2]. Depending on the operating point, the fuel temperature varies significantly.

For Kerosene being a low viscosity fluid, the fuel temperature influences atomization mainly by a reduction of surface tension. According to Rachner [3] the relation is

$$\sigma(T) = 1.550388E-05 \bullet (684.26 - T)^{1.222222} \quad (1)$$

where σ is the surface tension and T the temperature in Kelvin. For the purpose of this investigation, with it's limitation on 9 bar air pressure, the influence of solubility of air in Kerosene on surface tension at higher pressures is neglected in a first approximation. A correlation for the Sauter mean diameter of jets in crossflow at elevated pressures was given by Jasuja [4] which is represented here without the viscosity term

* Corresponding author: Christoph.Hassa@DLR.DE

$$\frac{SMD}{D} \propto \left(\frac{\sigma}{\rho_A U_A^2} \right)^{0.45} \bullet \left(1 + \frac{1}{AFR} \right) \tag{2}$$

where ρ_A is the air density, U_A the velocity of the cross flowing air and AFR the air to fuel ratio. Combining equation (1) and (2) allows a first guess of the influence of the kerosene temperature on atomization. In the same rig as used for this contribution, Becker [5] also investigated jets in cross flow and arrived at a dependency

$$SMD \propto C \bullet \left(\rho_A U_A^2 \right)^{-0.24} \tag{3}$$

for Kerosene and air at room temperature.

Kerosene being a multicomponent fuel has a distillation curve rather than a fixed boiling point and some segregation of components is inevitable during the process. However to make the problem amenable to a quick calculation Rachner [3] presented a formula for the specific enthalpy of vaporization for a constant mixture depending only on temperature

$$r(T) = 33339.03 \bullet (684.26 - T)^{0.38} \tag{4}$$

with r given in kJ/kg and the temperature in K.

In a previous investigation of a flat prefilming atomizer in the same rig, the fuel temperature was measured on the filmer plate by an insulated thermocouple [6]. Kerosene temperatures varied rather linearly over a wider range from 140 to 210 °C for an air temperature variation between 650 and 850 K. This was one of the reasons why the flat prefilmer showed a better performance than the jet in cross flow without fuel preheat of [5] with respect to atomization and evaporation.

Experimental Methods

Test Facility

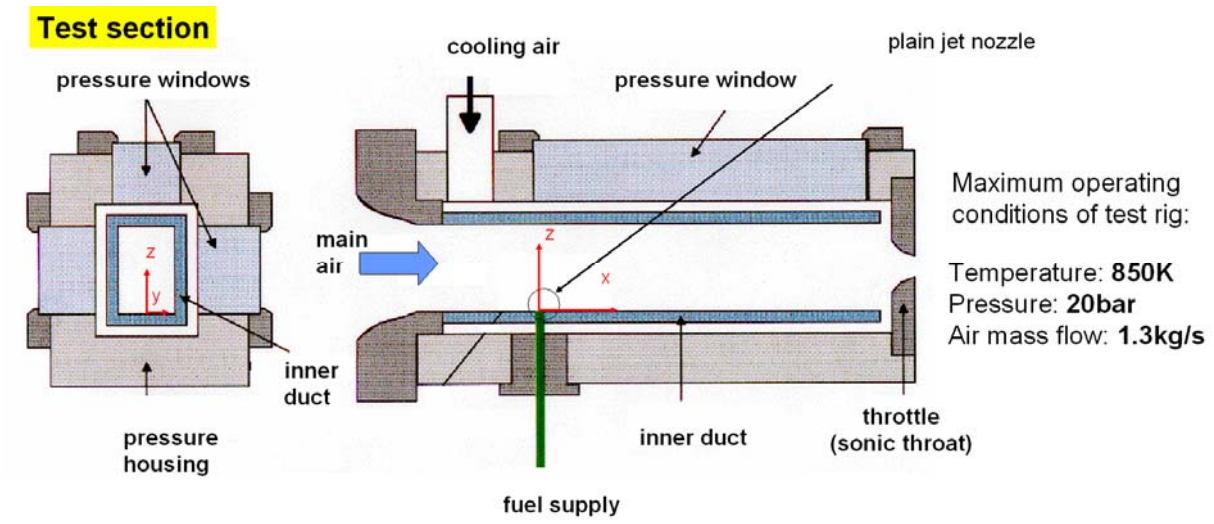

Figure 1 Schematic representation of the test section

The prevaporizing channel schematically represented in Figure 1 consisted of an inner glass channel with a cross section of 25 by 40 mm and 255 mm length. The pressure casing has three way optical access. On the fourth side, two atomizer ports allow to vary the residence time. Air from a 520 kW electrical heater can be preheated up to 850 K. The maximum air pressure is 20 bars, the maximum air mass flow 1.3 kg/s and the maximum fuel mass flow is 10 g/s, see [5], [6] and [7]. The operating parameters of the rig were held within an operating window, which was ±0.15 bar for the air pressure, ±2.5 K for the air temperature, ±2 m/s for the air velocity and ±2 % for the liquid mass flow.

The injector is made from high temperature steel, Figure 2. Its outer diameter is 5 mm and 2.5 mm on the last 5 mm's. The diameter of the fuel outlet is 0.45 mm being a practical lower limit to prevent clogging. To minimize residence time between preheater and injection, the injector l/d is far greater than 10. A Ni-Ni-Cr ther-

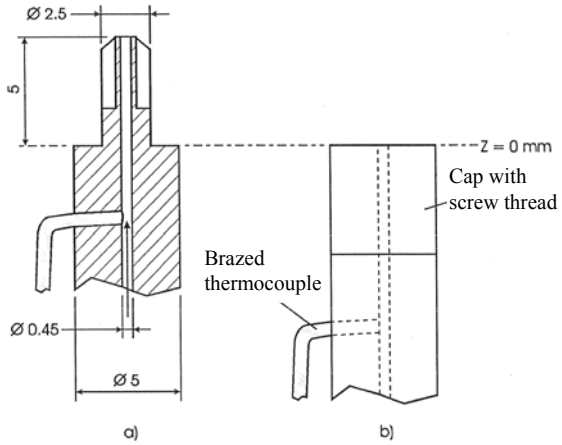

Figure 2 Injector representation for a) PDA, VIS-IR and b) Shadowgraphy

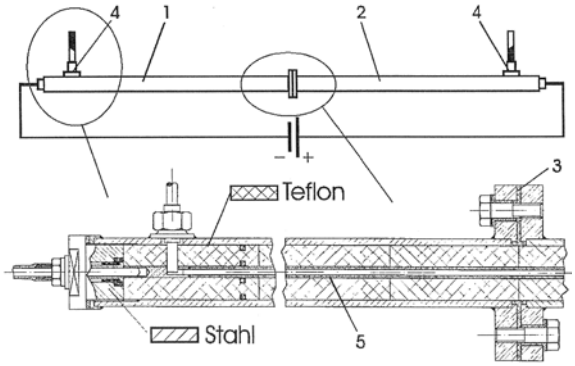

Figure 3 Kerosene heater

mocouple measures the fuel temperature 8 mm from the outlet. For reasons of optical access, the injector protruded 5 mm in the gas stream for PDA and VIS-IR measurements and was mounted flush for shadowgraphy.

The kerosene heater represented in Figure 3 was built specifically for the investigation. The fuel is guided by Ermeto fittings (4) through a tube (5) made of V_2A stainless steel with an outer diameter of 2 mm, a wall thickness of 0.2 mm and 2 m length, resulting in an electrical resistance of 2 Ω. The outer casing consists of two identical parts (1), (2) separated by a Teflon isolator disk (3). A maximum fuel pressure of 30 bars is allowed. The space between the tubes is filled with isolating material. The tube is electrically heated. The temperature control is effected by a control transformer with secondary voltage continuously variable from 0 to 280 V. Due to the low resistance of the heater tube, a secondary transformer is used to augment the current to 22 A. In the tandem configuration it can be operated with a maximum electrical power of 960 VA. The thermal efficiency was measured with 65 %. With a Kerosene mass flow of 2 g/s, kerosene blockage was registered between 150 and 160 °C, such that the experimental programme was limited to 150 °C.

Measurement techniques

The general behaviour of the spray was recorded by shadowgraphic imaging. The spray was illuminated through a condensing lens by a Nanolite with a flash duration of 100 ns. The shadows of the spray were imaged with a middle format camera Rolleiflex 6x6 using 80 mm focal length for global views and 50 mm for the near field. The shutter speed was 1/15 s such that the room had to be dark during the tests. At air speeds of 120 m/s the pulse duration is not quite short enough to freeze single droplets but sufficient to resolve the spray structure.

The qualitative distribution of the evaporated spray was measured with a line of sight technique using absorption of visible and infrared laser light thereby isolating the absorption of the fuel vapour as described in [8]. Collinear He-Ne lasers beams with 2 mW at 3.39 µm and 5 mW at 633 nm were used. The beam diameter in the measurement volume was 80 µm. The visible light was guided to a silicon diode and the infrared light to a lead sulphide detector. For background suppression the light was chopped at 120 Hz and amplified by a Lock-in amplifier. A detailed discussion of measurement errors of the used setup for Kerosene within the investigated operating conditions is given in [9]. Although absolute values for Kerosene cannot be calculated without using detailed spectroscopic information, the conclusion is that the uncertainty of comparisons between measurements for the same air temperature, i.e.750 K in this investigation, can be limited to 20%.

Droplet velocities, sizes and volume fluxes were measured with Phase Doppler Anemometry by Dantec. A standard PDA two component optic and a covariance processor were used [10]. The Laser beams of the Argon Ion Laser leaving the sending optics had 25 mW in the green beams measuring size and velocity and 30 mW in the blue beams. The focal length of sending and receiving optics were 310 mm, the fringe spacing was 9 µm. The diameter of the measurement volume was 80 µm. Although Brewster's angle for Kerosene is at 69°, a scattering angle of 52° had to be used to accommodate the receiving optics. Reflected light was additionally rejected by limiting the phase range of the photo detector pair U13 to 190° limiting the size range to 100 µm, the biggest 90% volume undersize diameter D_{V90} being measured with 35 µm.

The effects of the fuel temperature on the PDA measurement are fully described by the refractive index of the Kerosene droplet. Since the relative velocity is high for the heating period, the rapid mix model applies for the convective flow within the droplet and the temperature can assumed to be sufficiently uniform. The refractive index of Kerosene was determined experimentally in [11] for pressures of 1, 9 and 20 bars with and without scavenging convection up to complete evaporation. For the relevant 9 bar case with convection, the refractive index sinks from 1.45 at room temperature to 1.37 at the temperature corresponding to 95% evaporation. For the

used optical setup, this corresponds to a droplet measured 3.5% too high. For this investigation, the more relevant temperature interval is 40 to 150°C and it gives a difference of refractive index between 1.445 and 1.395 resulting in an error of 2.1%. The liquid volume flux measurements vary accordingly with 11 and 6.5 %. The effect is important compared with the other sources of error in the diameter measurement but does not invalidate the conclusions since the effect of fuel temperature on drop size and evaporation is systematically underestimated.

The liquid volume flux measurement used an in house algorithm described in [12]. Since the flow at the flux measurement positions was nearly one dimensional, only one component was used. The detection of the measurement volume size follows the basic ideas of Saffman [13] with a correction for the influence of the slit in the receiving optics from [12].

Measurement errors in the droplet velocities were calculated with geometrical errors and processor resolution to ±1.25 %. For the droplet size measurement, errors from the nonlinearity of the phase relationship were smaller than 1 µm. Uncertainties of the optical parameters of the setup lead to a maximum error of 3 %. Compared to combusting and swirling flows, the volume flux measurement finds more benign conditions as the flow is almost 1-D and the deterioration of the beam quality is less important due to the nearly isothermal gas flow and lower gas turbulence. Hence high signal to noise ratio's settings can be realized with the processor without loosing validation rate in a significant way. The most important impediment is the high concentration of the spray in the jet plume. The maximum throughput of the processor is 140 KHz. Due to the uneven statistics of particle arrival, losses begin to be significant before that value. Therefore a correction was introduced based on the statistical model of [14] presuming Poisson statistics. However the correction cannot work if significant loss of data occurs because of degrading signal to noise caused by the dense spray. Consequently unphysical increases of integrated volume flux occur between the measuring planes 15 and 30 mm behind the atomizer and for slowly evaporating sprays even between 30 and 60 mm. For the evaporating sprays at hand it means that reliable volume flux measurements are only possible when two thirds of the spray is evaporated. However at the 60 mm plane, data rates are below 100 kHz and acceptance rates above 90 % such that those measurements are held to be quantitative. In [9] tests without evaporation were made with several fuel flows around 1g/s. The nominal flow was always recovered with less than 10% diversion provided the data rate was small enough. For the current measurements with evaporation, a 15 % error for the volume flux is estimated for those measurements. Since the effect of fuel temperature is quantified by a difference of integrated values, systematic errors like loss of data or errors due to a diversion of refractive index partly cancel out.

Results and Discussion

Measurement programme

Table 1 PDA measurement conditions and PDA results integrated for the measurement planes.

	T_K [°C]	T_A [K]	p_A [bar]	u_A [m/s]	$\dot{m}_K$ (x=0) [g/s]	x [mm]	ρ_K (x=0) [kg/m³]	$\dot{m}_K$ (x) [g/s]	Evaporated [Vol-%]	SMD [µm]	$D_{0.1}$ [µm]	$D_{0.5}$ [µm]	$D_{0.9}$ [µm]	Number of Meas. Points
1	40	750.0	9.0	120	2.05	30	790.28	0.595	70.96	17.19	11.57	17.39	30.10	42
2	40	750.0	9.0	120	2.05	60	790.28	0.620	69.75	14.59	9.76	15.16	22.71	72
3	40	750.0	9.0	120	2.05	95	790.28	0.368	82.04	14.52	9.67	15.20	22.27	72
4	85	750.0	9.0	120	2.05	30	755.77	0.419	79.59	16.36	10.99	16.56	28.58	45
5	85	750.0	9.0	120	2.05	60	755.77	0.342	83.30	13.87	9.33	14.35	21.04	72
6	85	750.0	9.0	120	2.05	95	755.77	0.157	92.32	14.13	9.55	14.68	21.20	72
7	130	750.0	9.0	120	2.05	10	720.52	0.172	91.63	14.46	9.63	15.38	21.96	45
8	130	750.0	9.0	120	2.05	15	720.52	0.233	88.66	15.78	9.98	16.19	31.97	30
9	130	750.0	9.0	120	2.05	30	720.52	0.274	86.64	14.93	10.03	15.18	24.06	45
10	130	750.0	9.0	120	2.05	60	720.52	0.157	92.36	13.76	9.54	14.13	20.08	72
11	130	750.0	9.0	120	2.05	95	720.52	0.030	98.54	14.61	10.39	14.92	20.54	72
12	150	750.0	9.0	120	2.05	30	704.52	0.213	89.60	14.79	10.06	15.00	23.58	54
13	150	750.0	9.0	120	2.05	60	704.52	0.089	95.66	13.69	9.58	13.99	19.58	72
14	150	750.0	9.0	120	2.05	95	704.52	0.012	99.43	13.90	9.84	14.26	19.48	72
15	150	750.0	9.0	94	2.05	30	704.52	0.544	73.44	15.99	10.79	16.32	25.49	42
16	150	750.0	9.0	94	2.05	60	704.52	0.474	76.88	15.93	10.83	16.50	24.10	72
17	150	750.0	9.0	94	2.05	95	704.52	0.163	92.08	16.52	11.47	17.02	24.14	72
18	150	759.0	17.5	94	2.05	95	704.52	0.004	99.78	14.05	9.62	14.59	20.65	72
19	40	288.2	3.5	120	2.05	95	790.28			21.01	13.97	21.85	34.92	25
20	85	288.2	3.5	120	2.05	95	755.77			19.78	12.88	20.54	33.86	25
21	130	288.2	3.5	120	2.05	95	720.51			19.62	12.80	20.18	39.37	25
22	150	288.2	3.5	120	2.05	95	704.52			19.70	12.82	20.30	46.74	25
23	150	288.2	3.5	94	2.05	95	704.52			22.01	14.49	23.07	36.82	25
24	150	288.2	6.8	94	2.05	95	704.52			21.41	14.11	22.33	36.33	20
25	40	313.2	3.8	120	2.05	95	790.28			20.15	13.35	20.97	33.26	9
26	85	358.2	4.3	120	2.05	95	755.77			17.85	11.53	18.47	31.26	9
27	130	403.2	4.8	120	2.05	95	720.51			16.32	10.55	16.62	32.87	9
28	150	423.2	5.1	120	2.05	95	704.52			15.68	10.14	15.84	35.06	9

Two basic sets of measurements were made with high air temperature at 750 K for evaporation measurements and with an air temperature of 288 K respectively a temperature equal to the preheated fuel temperature and constant air density to monitor atomization with measurements in the far field of the injector. Because of the high particle concentration in the cold condition, measurements were only made at x =95 mm. Fuel temperatures were varied between 40 and 150 °C. The air pressure was 9 bar for the hot flow and chosen such that the air density remained the same for the cold conditions to preserve all atomizing conditions with the exception temperature. A variation of pressure to 17.5 bar and air velocity from the standard 120 m/s to 94 m/s were done for some hot conditions and the cold condition. The measurement planes were scanned with a grid size of 2.5 mm in y and z direction. Except for the fringe of the spray, the sample size was 10,000 such that the statistical basis for the mean values at x= 60 mm was about 5 million samples. The density was calculated with an expression from [3]:

$$\rho_K = a + b\,T_K + \frac{c}{d - T_K} \tag{5}$$

with a = 1034.227 kg/m^3, b = -0.70676104 kg/m^3/K, c = -9.488.259 kgK/m^3, d = 733 K.

Measurements of vapour absorption were made for all hot test conditions. The beam was scanned at the axial positions, here at 60 mm at lines of z = const. for every mm from y = 1 mm up to the position without absorption. The integration time was 10 s.

Results

First some shadowgraphic images are presented to provide a general impression of the flowfield. They were made at room temperature without preheating the fuel. Figure 4 is near the baseline case with equivalent density, Figure 5 near the case with lower air velocity and consequently higher penetration.

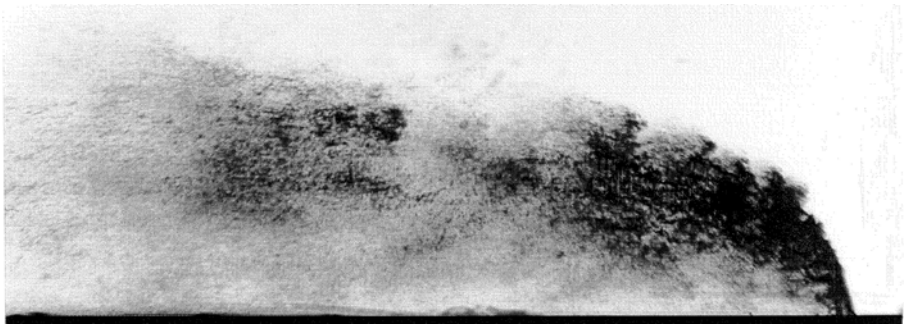

Figure 4 U_A=120 m/s, P_A=3.42 bar, m_K =2.05 g/s, left edge of image at x = 16 mm

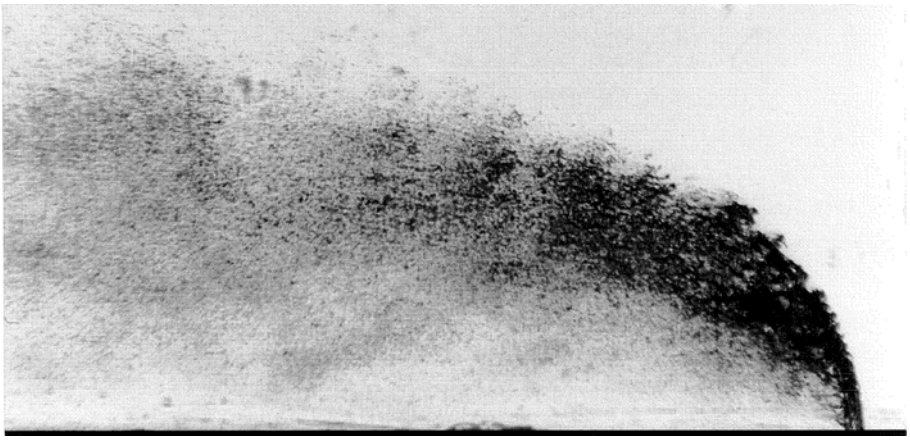

Figure 5 U_A=80 m/s, P_A=3.42 bar, m_K =2.05 g/s, left edge of image at x = 16 mm

According to the criterion of Wu et al. [15] for the division between column and surface breakup, the lower velocity in Figure 5 should be column breakup and the high velocity in Figure 4 should be a borderline case. However, inspection of the Figures rather suggests surface breakup for both cases. Since because of the long thin liquid passage of the injector, the velocity profile of the jet is rather far from a block profile, the effective momentum flux ratio will be higher, such that, according to Wu's expression, both points shift towards surface breakup.

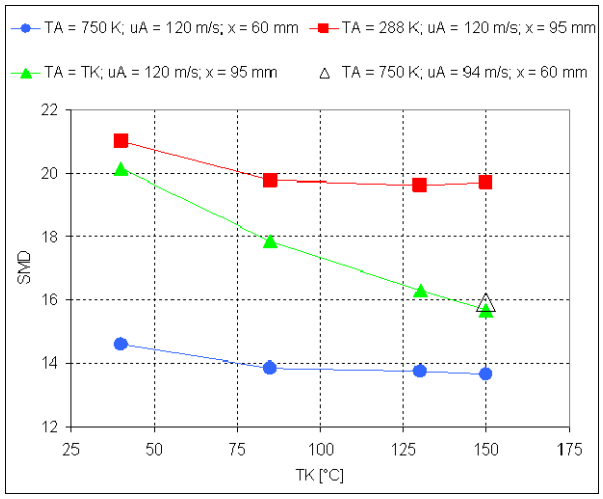

Figure 6 Sauter mean diameters over initial fuel temperature

Drop size measurements are presented for the cold cases at the measuring plane of x = 95 mm where the number concentration decreased sufficiently to allow measurements. For the hot case x = 60 mm is a compromise between the end of acceleration avoiding nonspherical droplets and nonrepresentative droplet samples due to an evaporation already progressed too far. The measurement points of table 1 represented in Fig. 6 are a volume flux averaged value for the measurement planes. The three cases with variation of fuel temperature are displayed: Equal fuel and air temperature, hot and cold air temperature. First the result of the concurrent variation of fuel and air temperature for the benchmark condition is commented, Figure 6. Between 40 and 150 °C, the SMD decreases from 20 to 16 µm. The proportionality to the fuel temperature is SMD ~ $T_K^{-0.84}$ with eq. (1) the proportionality to the surface tension follows with SMD ~ $\sigma_K^{0.59}$. This value is higher than the one in eq. (2), but with respect to the spread of the SMD this makes only a 10 % difference. However there are uncertainties in the drop size measurements and above all in the drop size correlations. In the review of [16], the bandwidth of exponents for the Weber number in the correlations for airblast atomization was given with an interval of $0.35 < x < 0.6$. Although it can be assumed, that an additional influence of the fuel temperature on the solubility of air in Kerosene at the investigated air pressures is present, thereby further reducing surface tension, the limited confidence in the drop size correlations and the measurement uncertainties do not enforce to use something more sophisticated than equation (1) for first order calculations.

The curve for the equal fuel and air temperature case lies in between the high and low air temperature case. Inspection yields two prominent features. Firstly, the influence of the air temperatures is even more prominent than the influence of the initial fuel temperature and secondly, the influence of the fuel temperature seems to vanish above 80°C preheat. The reason for the first phenomenon is most likely the heat transfer before and during atomization. It is evident that at the windward side of the jet but it must be important at all surfaces with high relative velocity, heating up or cooling the liquid boundary layer and thus lowering or rising surface tension before and during atomization.

The flattening of the curves with fuel preheat is less easy to explain. For the hot air case, a quasi-steady condition arises, when the final boiling temperature is approached at the surface before atomization. For the cold air case, the reason for the flat SMD curve can be found in a rise of the D_{90} values for the higher Kerosene preheat temperatures of 130 and 150 °C (line 21 and 22 in table 1), rising from 34 µm at 80 °C (line 19 in table 1) to 40 and 47 µm respectively. The rise at the big particle end compensates smaller diameters in the rest of the distribution. The results for the D_{90} were reproduced upon repetition of the measurements. No easy explanation is at hand. The same phenomenon was seen to a lesser degree for the equal fuel and air temperature measurements with the D_{90} rising from 31(line 26) to 33 (line 27) and 35 µm (line 28), and here heat transfer giving rise to temperature gradients in the liquid phase cannot play a role.

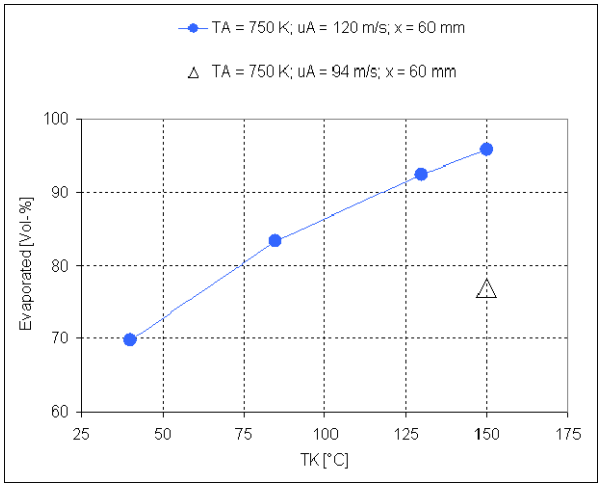

Figure 7 Spray evaporation against fuel preheat temperature

Variations of air pressure and velocity were only undertaken at the highest fuel preheat temperature with measurements only at x = 95 mm (lines 22 to 24). For the high pressure case, less than 1% of the spray remains at that station, hence drop sizes are not reported. For the lower velocity (line 23), the SMD rises from 14 to 16 µm. Comparing with eq. (1) and (2), the velocity influence is in between the two correlations and not surprisingly nearer to eq. (2) which was measured for a very similar case.

The evaporation measured by the comparison of the sampled against the initial liquid volume at x = 60 mm is displayed in Figure 7. There is a clear tendency of higher evaporation with a difference of 26 % between the lowest and highest Kerosene preheat temperature for the nominal residence time of 0.5 ms. The gradient of the evaporation curve becomes smaller above 80 °C, which is inline with the SMD curve for

the condition, where no further size reduction was seen above that temperature. Thus the gradient below 80 °C represents the combined effect of size reduction and preheat on evaporation, whereas the gradients in the upper part isolate the effect of the Kerosene preheat. The evaporation measured for the air velocity of 94 m/s illustrates the effect of the dropsize. A difference of 2 µm or 15 % in SMD effects 19 % higher vaporization at the x = 60 mm station.

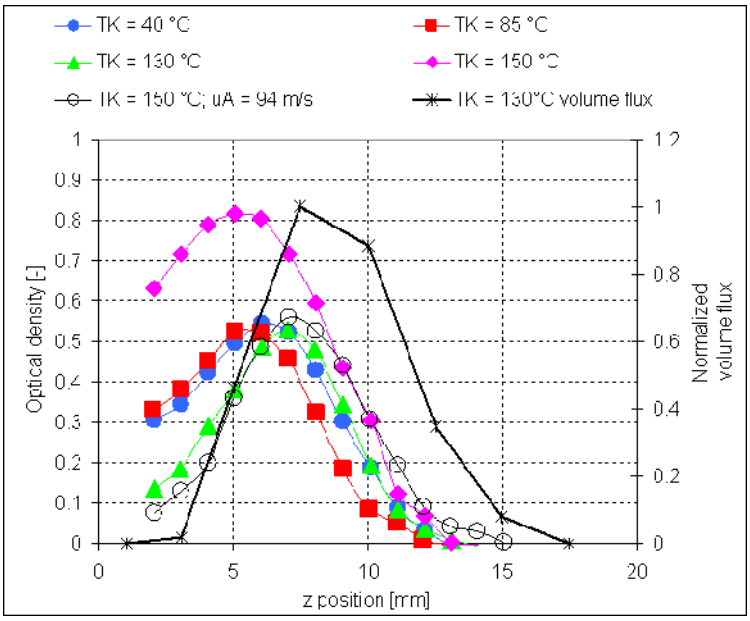

Figure 8 Optical density of Kerosene vapour and normalized liquid volume flux at x = 60 mm

Finally the results from the VIS-IR absorption measurements at x = 60 mm will be presented in Figure 8. For comparison, a normalized curve of the liquid volume flux for the air velocity of 120 m/s and 130 °C fuel preheat is presented. The most apparent feature is the difference in penetration between the liquid volume flux and the vapor absorption profiles for the same air velocity of U_A = 120 m/s and hence momentum flux ratio. This difference is not apparent at the first measurement planes of x = 10 and 15 mm but only evolves downstream, when the peak of the volume flux continues to move vertically and the peak of the optical density doesn't. Here it has to be kept in mind, that a flux is compared with a density proportional to vapor concentration. Compared to the flux, the concentration rises in the regions with low velocity near the wall or in the wake of the jet. The different penetration behavior for the two momentum flux ratio's which can be seen in Figures 4 and 5 is also recognized in the comparison for the optical density curves of the 150 °C preheat for U_A = 120 (diamond) and U_A = 94 m/s (hollow circle). For the higher liquid momentum flux of Fig. 5, spray and vapor detaches from the wall, whereas for the lower momentum flux, parts of the spray remain near the wall, Fig. 4., and the optical density of the vapor remains high for the measurement point nearest to the wall. It can be assumed, that this behavior strongly depends on the atomization mode. A quicker onset of shear atomization by Kerosene heating can be expected. For shear breakup, liquid is sheared off the jet boundary layer early on and quickly loses vertical momentum because of the short stop distance of the produced droplets. Hence in this case there is a vertical separation between the droplets produced by shear break up and the remaining jet atomized by column break up. Naturally evaporation progresses faster for the liquid atomized early and here we see a notable influence of the fuel preheat. Whereas the optical density curves for the different fuel preheats stay close to each other on the windward side, there is stratification towards the wall with considerable enrichment for higher fuel preheat. Unfortunately the behavior of the optical density curves with temperature is not steady or even monotonic. The curve for 130°C is shifted to the positive z direction by about 2 mm and has a lower optical density near the wall. Since this is the case for all axial measuring positions, this is judged to be an error in the setting of the fuel flow and hence momentum flux. Nevertheless there seems to be a clear qualitative trend for the other temperatures.

Summary and Conclusions

The goal of this contribution is to provide information on the magnitude of the effect of fuel preheat in gas turbine combustors with partial prevaporization and premixing. Due to the high Weber number of the atomization process and the complexity of the fuel, experimental information is needed. Since the magnitude of the effect is closely coupled to droplet size, realistic operating conditions with respect to the parameters influencing atomization are required. The extent to which this is also the case for other parameters influencing evaporation, namely temperature and fuel was one of the questions to be answered by this study and hence the influence had to be reproduced in the experiment. The resulting environment poses challenges to the use of optical techniques, the number density of droplets of the resulting fine spray for the application of PDA and the ill-definedness of Kerosene for the application of the vapor absorption techniques. Nevertheless, the experimental techniques were clearly able to identify the trends in a meaningful manner. To the author's knowledge, this is the first study to expose them at realistic operating conditions, specifically at a typical aero engine cruise condition.

With respect to the influence of fuel preheat on drop size, the capability of the vaporizing duct to independently vary air pressure as well as fuel and air temperature enabled to investigate the influence of temperature

isolated from density and heat transfer effects. Using equation 1, it could be concluded, that for Kerosene with the experimental uncertainties connected to drop size correlations, the influence is indeed sufficiently described by surface tension. However, the variation of fuel temperature and constant high and low air temperature shows that the real question is how to define that surface tension and no easy answer is at hand. Instead it has to be concluded, that heat transfer from the hot air to the liquid prior to and during atomization always influences atomization in a way not to be neglected as demonstrated by the large difference of the drop sizes for high and low air preheat at constant air density and velocity, which surpasses the influence of the fuel preheat. Obviously this has implications for the detailed modeling of atomization processes.

The influence of the 110°C fuel preheat on drop size at high air temperature was smaller than the difference effected by the air velocity variation from 94 to 120 m/s. However the reverse is observed for the influence on evaporated mass at the measurement section of 60 mm, where the fuel preheat led to 26% more evaporated fuel. This is obviously due to the reduced enthalpy needed for evaporation and is a sizeable effect compared with the difference in pressure loss needed to accelerate from the lower to the higher velocity. The higher vaporization rate will influence the flame position in real combustors and will be especially important in situations when flame stability or combustion efficiency is marginal.

The enrichment of fuel vapor observed in the wake of the jet for the lower penetration case is certainly tied to the occurrence of special conditions which are not always present, but it shows that the fuel preheat can give rise to a behavior which could influence flame stabilization in a nonlinear way as in this case where especially the amount of vapor produced early in the vaporization process is influenced. This is not necessarily limited to shear breakup of jets in cross flow, as an analog situation occurs for the atomization from the wave crests of prefilming atomizers.

Generally the results show that the effects of increased initial fuel temperature are big enough to justify an investigation in a more realistic environment with combustion where the changes in combustion behavior and performance could be studied.

Acknowledgements

Partial funding by EU under contract number BRPR-CT95-0122 is gratefully acknowledged. Furthermore, the authors would like to thank Sebastian Cordes for the development of the Kerosene preheater and Stefan Freitag for help with the error analysis and the graphics.

References

[1] Anon.: The jet engine, *Rolls Royce*, ISBN 0902121235 (1986).

[2] Stickles R.W. et al.: Fuel injector design for high temperature aircraft engine, Fuels *and Combustion Technology for Advanced Aircraft Engines*, AGARD Conference Proceedings 536, Paper 20 (1993).

[3] Rachner, M.: Die Stoffeigenschaften von Kerosin Jet A-1, *ISRN DLR-FB-98-01* (1998).

[4] Jasuja, A.K.: Plain-jet air blast atomization of alternative liquid petroleum fuels under high ambient pressure conditions, *Technical Paper 82-GT-32, ASME* (1982).

[5] Becker, J., and Hassa, C.: Breakup and atomization of a kerosene jet in cross flow at elevated pressure, *Atomization and Sprays,* 14:15-35 (2002).

[6] Brandt, M., Gugel, K.O., Hassa, C.: Experimental investigation of the liquid fuel evaporation in a premix duct for lean premixed and prevaporized combustion, *Journal of Engineering for Gas Turbines and Power*, 119: 815-821 (1997).

[7] http://www.dlr.de/at/en/desktopdefault.aspx/tabid-1552/2449_read-3813/

[8] Winklhofer, E., Plimon, A.: Monitoring of hydrocarbon fuel-air mixtures by means of a light extinction technique in optically accessed research engines, *Optical Engineering*, 30: 1262-1268 (1990).

[9] Brandt, M.: Lasermesstechnische Untersuchung der Kerosinverdampfung und -mischung für die magere Vormischverbrennung unter erhöhtem Druck, *DLR Forschungsbericht* 1999-25, ISSN1434-8454 (1999).

[10] Anon.: PDA user's manual, *Dantec, Skovlunde Denmark* (1992).

[11] Fitzky, G. and Bohn, D.: Messung der komplexen Brechungsindizes von Heizöl EL und Kerosin in Abhängigkeit von Druck und Temperatur, *Forschungsbericht,* Lehrstuhl und Institut für Dampf- und Gasturbinen, RWTH Aachen (1995)

[12] Brandt, M.: Liquid and gaseous fuel measurements in a premix duct, *11th.European Conference of ILASS-Europe on Atomization and Sprays,* ed. Bauckhage, ISBN 3-921590-34-5 (1995).

[13] Saffman, M.: Automatic calibration of measurement volume size, *Applied Optics,* 26: 2592-2597 (1987).

[14] Edwards, C.F., Marx, K.D.: Application of Poisson Statistics to the Problem of Size and Volume Flux Measurements by Phase Doppler Anemometry, *ICLASS-91, Gaithersburg, USA* (1991).

[15] Wu, P.K., Kirkendall, K.A., Fuller, R.P., Nejad, A.S.: Breakup process of liquid jets in subsonic cross flows. *Journal of Propulsion and Power* 13:64-73 (1997).

[16] Winterfeld, G., Eickhoff, H., Depooter, K.: Fuel injectors, *Design of modern turbine combustors*, ed. Mellor, A.M., *Academic Press*, London (1990).